

# Accepted Manuscript

The experimental evaluation and improvements of a novel thermal diode pre-heat solar water heater under simulated solar conditions

M. Smyth, P. Quinlan, J.D. Mondol, A. Zacharopoulos, D. McLarnon, A. Pugsley



PII: S0960-1481(17)31283-1

DOI: [10.1016/j.renene.2017.12.083](https://doi.org/10.1016/j.renene.2017.12.083)

Reference: RENE 9580

To appear in: *Renewable Energy*

Received Date: 11 October 2017

Revised Date: 20 December 2017

Accepted Date: 22 December 2017

Please cite this article as: Smyth M, Quinlan P, Mondol JD, Zacharopoulos A, McLarnon D, Pugsley A, The experimental evaluation and improvements of a novel thermal diode pre-heat solar water heater under simulated solar conditions, *Renewable Energy* (2018), doi: 10.1016/j.renene.2017.12.083.

This is a PDF file of an unedited manuscript that has been accepted for publication. As a service to our customers we are providing this early version of the manuscript. The manuscript will undergo copyediting, typesetting, and review of the resulting proof before it is published in its final form. Please note that during the production process errors may be discovered which could affect the content, and all legal disclaimers that apply to the journal pertain.

# The experimental evaluation and improvements of a novel thermal diode pre-heat solar water heater under simulated solar conditions

\*M Smyth, P. Quinlan, JD Mondol, A. Zacharopoulos, D McLarnon and A Pugsley

*\*Centre for Sustainable Technologies, School of the Built Environment,  
Ulster University, Newtownabbey BT37 0QB, N. Ireland.*

Tel: ++44(0)2890368119, Fax: ++44(0)2890368239, e-mail: m.smyth1@ulster.ac.uk

## ABSTRACT

This paper presents the development through experimental performance characterisation of a pre-heat Integrated Collector Storage Solar Water Heater using a novel thermal diode operation to reduce ambient heat loss during non-collection periods. Using a solar simulator facility at Ulster University, the novel prototype pre-heat Mark IV unit was tested and evaluated. The concept has been designed and developed to be a sustainable pre-heat alternative to other types of solar water heating systems traditionally used in domestic hot water installations. The highest 6 hour collection efficiency was 36.17% under solar simulated conditions. The lowest system 'U' value was  $0.98 \text{ Wm}^{-2}\text{K}^{-1}$  with no draw-off conditions. When the current prototype ICS units are compared with other conventional ICS systems, particularly in terms of thermal retention during non-collection periods, an improved performance is clearly demonstrated. The measured thermal losses were approximately 40% less than other similarly measured systems.

## Keywords

ICSSWH, pre-heat, solar simulation, thermal diode

## 1 Introduction

The Energy Performance of Buildings Directive (EPBD) requires that Renewable Energy Systems (RES) are actively promoted in offsetting conventional fossil fuel use in buildings. A better appreciation of solar thermal system (STS) integration will directly support this objective, leading to an increased uptake in the application of renewables in buildings. Meeting building thermal loads will be primarily achieved through an extensive use of renewables, following standard building energy saving measures, such as good insulation or advanced glazing systems. Solar thermal systems are expected to take a leading role in providing the thermal energy needs, as they can contribute directly to the building heating, cooling and domestic hot water requirements.

Integrated Collector Storage Solar Water Heaters (ICSSWH) are simple, low cost solar devices and as such offer a suitable technology to partially meet the demands of the EPBD. The first ICSSWH systems consisted of exposed tanks of water left out to warm in the sun. Used on a few farms and ranches in the Southwest of the USA in the late 1800s, they were reportedly capable of producing water hot enough for showering by the late afternoon on clear days [1]. The first solar water heater, manufactured commercially under the trade name 'The Climax Solar-Water Heater' was an ICSSWH patented in 1891 [2]. The development of these systems is detailed in Smyth et al [3] and more recently by Singh et al [4], along with their tendency to suffer significant ambient

41 heat loss, especially at night-time and during non-collection periods. Many studies have been carried out focusing  
42 on the improvement of the thermal performance of ICSSWH systems, primarily during night operation [3][4].  
43 Double vessel configurations offer an interesting solution to mitigating this problem.

44

45 Kalogirou [5] presents work conducted on a double vessel ICS design, examining the role and potential benefits  
46 of a smaller pre-heat vessel inserted in the collector cavity, directly above the main vessel. Quinlan [6] and  
47 Souliotis et al [7] optically analysed and experimentally studied a heat retaining ICS vessel design (based on De  
48 Beijer's [9] double vessel concept) mounted horizontally inside a stationary truncated asymmetric compound  
49 parabolic concentrating (CPC) reflector trough, combining 3 heat retaining enhancements previously researched.  
50 The thermal behaviour of the ICS system was compared to that of a Flat Plate Thermosiphonic Unit (FPTU) and  
51 experimental results showed that the ICS system was as effective during daily operation as it was during the  
52 night. Furthermore, the thermal loss coefficient during night-time operation was similar for the ICS system and  
53 FPTU. The current work presented in this study fully details the experimental characterisation of a pre-heat  
54 ICSSWH that utilises the novel thermal diode operation first presented by De Beijer [9] and enhanced by  
55 Souliotis et al [7][8]. This study enhances and further develops the work presented by Smyth et al [10] on the  
56 experimental performance characterisation of a pre-heat ICSSWH that utilises the same novel double vessel  
57 thermal diode operation but characterised using a bespoke thermal flux simulation test facility. Specific areas of  
58 improvement include methods of improving Heat Transfer Fluid contact with the absorbing surface, internal  
59 vapour and condensate control and external insulation.

60

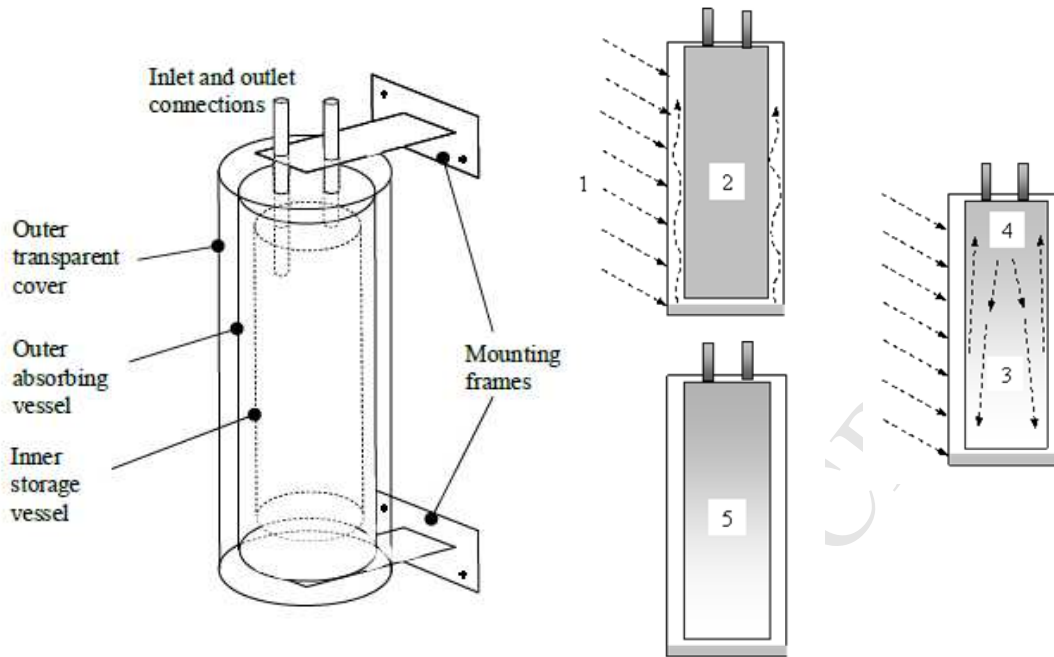
## 61 **2 Description of the pre-heat thermal diode ICSSWH**

62 The conceptual pre-heat thermal diode ICSSWH is fabricated using 3 concentric cylinders; one transparent  
63 polymer outer cylinder forming the aperture and unit casing to protect the absorber vessel coating and reduce  
64 convective heat loss as well as defining the initial physical appearance of the unit; the other two metal vessels  
65 combine to create the integral collector/storage element. The outer vessel is the solar absorber (with an inner  
66 evaporating surface) and the inner vessel is the thermal store (with a condensing outer surface). The concentric  
67 design of the two vessels defines the annular cavity, crucial to the thermal diode operation. The generic system  
68 design and operation is illustrated in Figure 1.

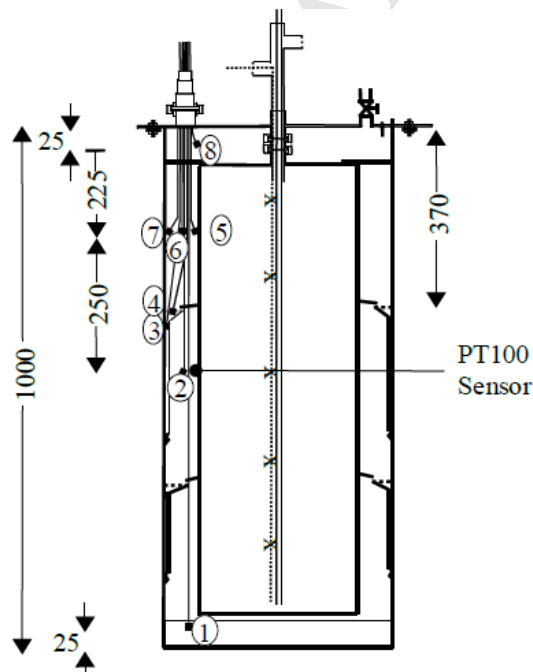
69

70 The annular cavity is partially evacuated to a low pressure ( $\sim 50\text{mb}$ ) and contains a small amount of a  
71 liquid/vapour PCM (phase change material) heat transfer fluid. This arrangement forms the thermal diode,  
72 promoting solar collection and thermal storage through phase change processes whilst reducing thermal losses by  
73 the vacuum insulation. During collection periods, solar radiation incident on the outer surface of absorbing vessel  
74 (the evaporator with selective coating) [pt 1] causes the PCM in contact with the vessel wall to evaporate at low  
75 temperature thus producing a vapour. The PCM vapour condenses on contact with the colder inner (storage)  
76 vessel (condenser) surface and the thermal energy is transferred to water store through latent heat exchange [pt  
77 2]. Condensed PCM runs down the vessel wall to a reservoir at base of the annulus to repeat the cycle [pt 3]  
78 whilst the temperature of the store stratifies [pt 4]. During non-collection periods no evaporation takes place (no  
79 incident energy to drive the evaporation process) and because of the insulating layer created by the annulus, heat  
80 loss is reduced from the store [pt 5]. The annular cavity can use a range of liquid/vapour phase change materials

81 (such as alcohols and commercial refrigerants), but water is the most cost effective and environmentally benign  
 82 material and was the PCM of choice for this study.



98 Figure 1: The initial conceptual design and operation of the pre-heat thermal diode ICSSWH



113 Figure 2: Cross section detail of the pre-heat thermal diode ICSSWH

114  
 115  
 116 A modified prototype version (Mark IV) of the pre-heat thermal diode ICSSWH was produced and evaluated  
 117 using the solar simulator facility at Ulster University. This prototype was designed to increase the solar collection  
 118 efficiency of previous 'base unit' designs developed by Quinlan [6]. By increasing the amount of Phase Change  
 119 Material Heat Transfer Fluid (PCM HTF) volume in the annular cavity that was in direct contact with the heated  
 120 absorbing (evaporator) surface of the outer vessel via a series of intermediate raised water reservoirs (pockets)  
 121 that were longer and thinner than previous reservoir designs it was projected that an improved performance

would result. In addition, adding a cowl configuration that was modified to permit upward flow of vapour but prevent downward flow of condensate (beyond the designated pocket) would also improve performance. Figure 2 depicts a cross sectional detail of the Mark IV thermal diode ICSSWH. The impact of these design modifications on the collection and cool down performance under solar simulated test conditions are presented. A number of different tests were conducted on the Mark IV prototype; exposed concentric cylinder design (MIV10), with outer transparent casing (MIV11) and outer transparent casing with insulation in the back 1/3 of the aperture cavity (MIV12). All variants had a starting annular cavity pressure at  $\sim 30$ mb which represented at relatively low vaporising temperature and was achievable with the vacuum equipment in the laboratory.

The base unit consisted of two vessels, the outer vessel was 300mm  $\varnothing$  (1m in length) and the inner vessel was 200mm  $\varnothing$  (0.9m in length). Both vessels were fabricated from 1.5mm thick stainless steel sheet. Each vessel had a welded base with a flanging arrangement to allow for access and entry for monitoring instrumentation. The other unit variants were based the same dimensional and construction features used in the fabrication of the control unit, but incorporated the outer transparent casing and/or back insulation. The outer transparent casing was made from 1mm thick PETG sheet with a stated transmissivity of 0.90 [11]. To increase radiation absorption, stove paint with absorptivity 0.95 [12] was applied to the outer vessel surface. The Mark IV had a mass of 24.16 kg, thermal mass of 11.3(kJ/K), outer vessel (absorbing) surface area of 1.08 m<sup>2</sup> and inner vessel volume of 28.2 litres.

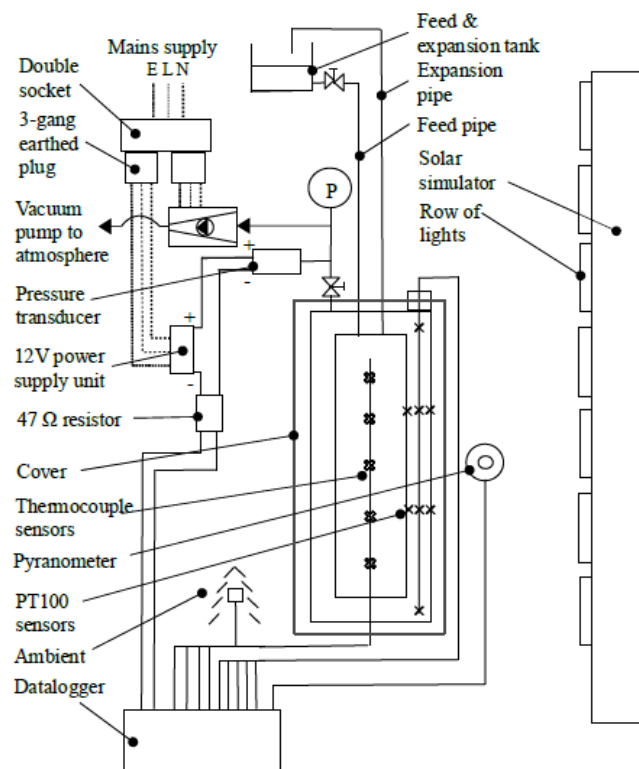


Figure 3: Schematic diagram of solar simulation test facility

### 3 Description of the experimental facility

The experimental performance of the Mark IV variant pre-heat thermal diode ICSSWH concept was determined using the state-of-the-art solar simulation facility at Ulster University. The indoor solar simulator testing facility

163 consisted of 35 high power metal halide lamps arranged in 7 rows of 5 lamps. Each lamp is furnished with a  
 164 rotation symmetrical paraboloidal reflector to provide a light beam of high collimation. In order to achieve  
 165 uniform distribution of light intensity on the test area, a lens is inserted in each lamp to widen the illumination of  
 166 light. The characteristic combination of the reflector, lens and lamps ensures a realistic simulation of the beam  
 167 path, spectrum and uniformity. The solar simulator control panel maintained the constant level light intensity  
 168 automatically on the collector surface via a datum CMP6 Kipp and Zonen pyranometer (mounted at the centre of  
 169 the test plane). T-type copper-constantan thermocouples were used to measure temperatures within the various  
 170 units, including vessel, store and surface temperatures and ambient air temperature. Water storage temperatures  
 171 were measured at eight locations to record the variation of water temperature within the inner store. Temperature,  
 172 pressure and radiation measurements were recorded through a Delta T logging device linked to a PC, as shown in  
 173 figure 3 and detailed in table 1.

174

175 Table 1: Details of experimental instrumentation

Measured Variable	Equipment	Range and Sensitivity
Temperature	T-type copper-constantan thermocouples	$\pm 0.5^{\circ}\text{C}$ between 0 and $70^{\circ}\text{C}$
Temperature	PT100 sensors	$\pm 0.5^{\circ}\text{C}$ accuracy with an experimentally determined standard deviation of $\pm 0.1^{\circ}\text{C}$ .
Solar radiation	CMP6 Kipp and Zonen pyranometer	directional error up to $80^{\circ}$ at $1000 \text{ W/m}^2$ was $< 20 \text{ W/m}^2$
Pressure	Druck DPI 104 digital pressure gauge	Gauge pressure between -1bar (vacuum) to 20bar at 0.05% FS ( $\pm 10\text{mbar}$ ).
Pressure	Danfoss MBS 33-2421-3AB05 pressure transmitter	Output of 4-20mA and an absolute pressure range 0 to 25 bar

176

177 **4 Description of the experimental procedure**

178 The collection and thermal retention performance characteristics for all units were determined under solar  
 179 simulated conditions. System performance characterisation was based on BS ISO 9459-5:2007 [13] applied to  
 180 indoor conditions and whole-system testing. No thermal storage draw off was performed during any of the tests in  
 181 this presented work. The tests were conducted over time periods of 6 to 24 hours in order to determine the daily  
 182 collection efficiency (6 hours solar simulator exposure with an average solar intensity of  $\sim 800 \text{ W/m}^2$ ) and an 18  
 183 hour cool down period to determine thermal retention. At the beginning of each experiment the inner vessel was  
 184 re-filled and the test started with stable ambient temperatures and uniform tank temperatures.

185

186 Figure 4 shows the prototype Mark IV rig prior to exposure. The collection phase started when the simulator was  
 187 switched on and a 30 minute warm up period elapsed. The prototype and test facility were then monitored for six  
 188 hours after which the simulator were turned off. The cool down phase started immediately after simulator switch  
 189 off and lasted for a further 18 hour period. Test information from the data logger was then downloaded for  
 190 analysis.

191

192

193

194

195

196  
 197  
 198  
 199  
 200  
 201  
 202  
 203  
 204  
 205  
 206  
 207  
 208  
 209  
 210  
 211  
 212  
 213  
 214  
 215  
 216  
 217  
 218  
 219  
 220  
 221  
 222  
 223  
 224  
 225  
 226  
 227  
 228  
 229  
 230  
 231  
 232  
 233

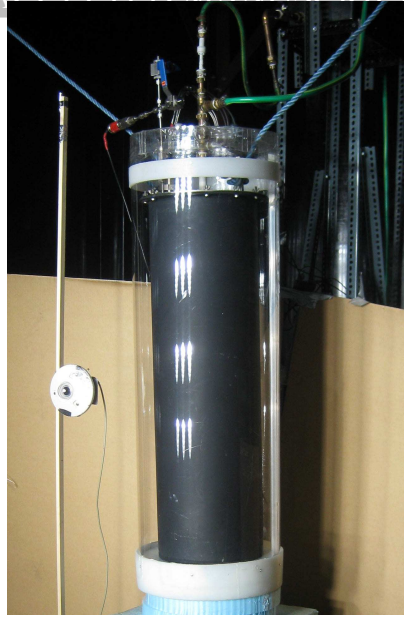


Figure 4: Images of the Mark IV unit under solar simulator test conditions

## 5 Analysis methods

The performance of each was experimentally determined from the data retrieved from the extensive testing programme. The thermal store, inner cavity/annulus and external environment in and around the collector aperture were examined during testing to define the system characteristics. The thermal store characteristics were retrieved from the average and normalised vessel temperatures and stratification during collection and cool down phases to create lumped collection and thermal retention efficiencies and develop the hypotheses for heat transfer mechanisms into and within the thermal store. The annulus characterisation used measured temperature and pressure variables taken during the collection and cool down phases, allowing review of temperature distribution and analysis of the sensible and latent heat transfer mechanisms taking place. The external environment is not characterised independently but as part of the characterisations within the thermal store and annulus. The following equations and terms are used. Simulated solar energy incident on the aperture area over the test period,

$$Q_{\text{incident}} = G_{\text{ave}} A_{\text{ap}} \Delta t \quad \{1\}$$

where

$$G_{\text{ave}} = \left( \int_{t_{\text{end}}}^{t_{\text{start}}} I(t) dt \right) / \Delta t \quad \{2\}$$

Experimentally measured temperatures were used to calculate average water temperatures in the thermal store volume ( $T_{\text{av}}$ ). The average start temperature ( $T_{\text{initial}}$ ) and average end temperature ( $T_{\text{end}}$ ) were determined during the collection phase using the recorded water temperatures in the thermal store at the beginning and end of collection period. Thermal energy collected ( $Q_{\text{col}}$ ) by the unit was determined by

$$Q_{\text{col}} = mc_p (T_{\text{end}} - T_{\text{initial}}) \quad \{3\}$$

234 The unit collection efficiency was determined by

235

$$236 \quad \eta_{col} = \left( \frac{Q_{col}}{Q_{incident}} \right) \times 100 \quad \{4\}$$

237

238 The collection efficiency varies depending on the collection time period used therefore during evaluation it was  
239 measured over a 6 hour period unless otherwise specified. Thermal stratification within the store is characterised  
240 by a stratification index ( $\sigma$ ) calculated using equation (5) [14]

241

$$242 \quad \sigma = \frac{(T_{av,t} - T_{av,b})}{(T_{av,t} - T_{av,b})_{start}} \quad \{5\}$$

243

244 where  $T_{av,t}$  and  $T_{av,b}$  are the average thermal store temperatures within the top 1/5 and bottom 1/5 storage volumes  
245 and  $(T_{av,t} - T_{av,b})_{start}$  is the temperature difference between the top 1/5 and bottom 1/5 storage volumes at the  
246 beginning of the collection phase. A de-stratification time constant measured as the time it takes for the  
247 stratification index  $\sigma$ , to decrease to 0.3679 of its initial value, is used to measure de-stratification during the cool  
248 down period. Thermal retention efficiency ( $\eta_{ret}$ ) is determined by

249

$$250 \quad \eta_{ret} = \left( \frac{m \times c_p (T_{final} - T_{amb})}{m \times c_p (T_{initial,c} - T_{amb})} \right) \times 100 \quad \{6\}$$

251

252 where  $T_{initial,c}$  is the average temperature at the start of the cool-down period,  $T_{final}$  is the average temperature at  
253 the end of the cooling period and  $T_{amb}$  is the average ambient temperature throughout the cool-down phase. The  
254 system heat loss coefficient also known as the system 'U' value was calculated from equation (7) [15]

255

$$256 \quad U_{system} = \frac{mc_{system}}{A_{unit} \Delta t} \ln \left( \frac{(T_{initial,c} - T_{amb})}{(T_{final} - T_{amb})} \right) \quad \{7\}$$

257

258 where  $mc_{system}$  is the thermal mass of the system based on the mass and specific heat capacity of the individual  
259 units and  $A_{unit}$  is the surface area of the outer vessel. All monitoring instrumentation has an associated  
260 experimental accuracy as presented in table 1.

261

## 262 6 Results and Discussion

263 Mark IV under solar simulation evaluated the base thermal diode ICSSWH concept at 30mb inner operating  
264 pressure as a bare unit (MIV10), a transparent cover (MIV11) and added insulation within the cover (MIV12).  
265 The 6 hour collection efficiencies for MIV10 and MIV12 under solar simulated test conditions were 29.39%  
266 and 36.17%, respectively. This was a marginal increase in collection performance and poor in overall terms.  
267 However, this work focuses on the importance of certain system features and subsequent designs have built upon  
268 this early work, resulting in even better collection efficiencies. Collection efficiencies, normalised average store



269 and annulus temperatures for the current work are shown in figures 5, 6, 7 and 8, respectively. The store  
 270 thermocline development, store stratification index, system 'U' values and retention efficiencies for MIV10 and  
 271 MIV12 are shown in figures 9, 10 and 11, respectively.

272

273

274

275

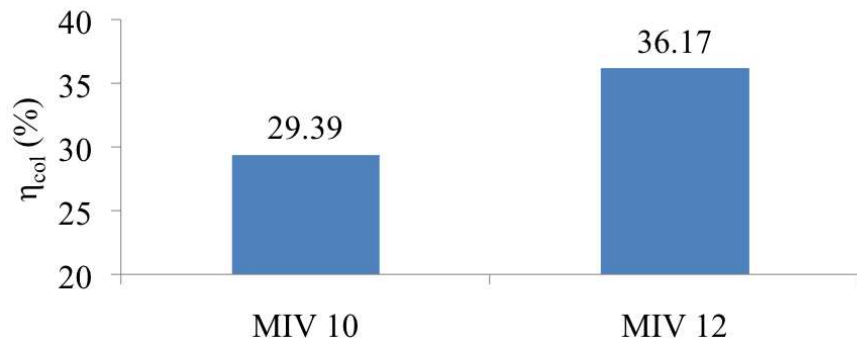
276

277

278

279

280



281 Figure 5: The 6 hour collection efficiencies for MIV10 and MIV12 under solar simulated test conditions

282

283

284

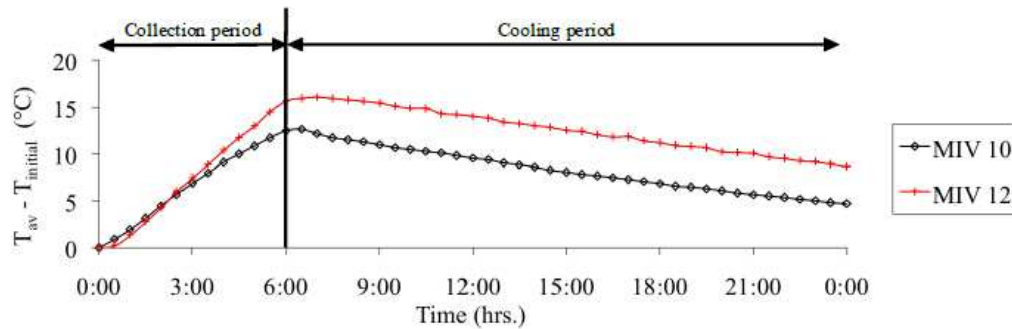
285

286

287

288

289



290

291

292

293

294

292 Figure 6: Normalised average vessel store temperature for MIV10 and 12 during a 6 hour collection period and  
 293 18 hour cool down period under solar simulated and indoor ambient test conditions

295 As shown in figure 5 (based on temperatures shown in figure 6), the 6 hour collection efficiency under the solar  
 296 simulator for MIV12 was 36.17% representing an increase of 23% over MIV10 due to the addition of 50mm  
 297 back insulation and transparent cover. Figure 7 illustrates the annulus temperatures and pressure for selected  
 298 Mark IV tests over a 6 hour collection period under solar simulation test conditions. From the initial starting  
 299 annulus pressure of ~30mb, a small rise of 50mb over the test period was observed due to the vapour creation in  
 300 the annulus. On the test end, the pressure was measured and in all cases was back to the starting pressure  
 301 indicating a hermetic seal was still present and all thermal measurements were due to system operation.

302

303

304

305

306

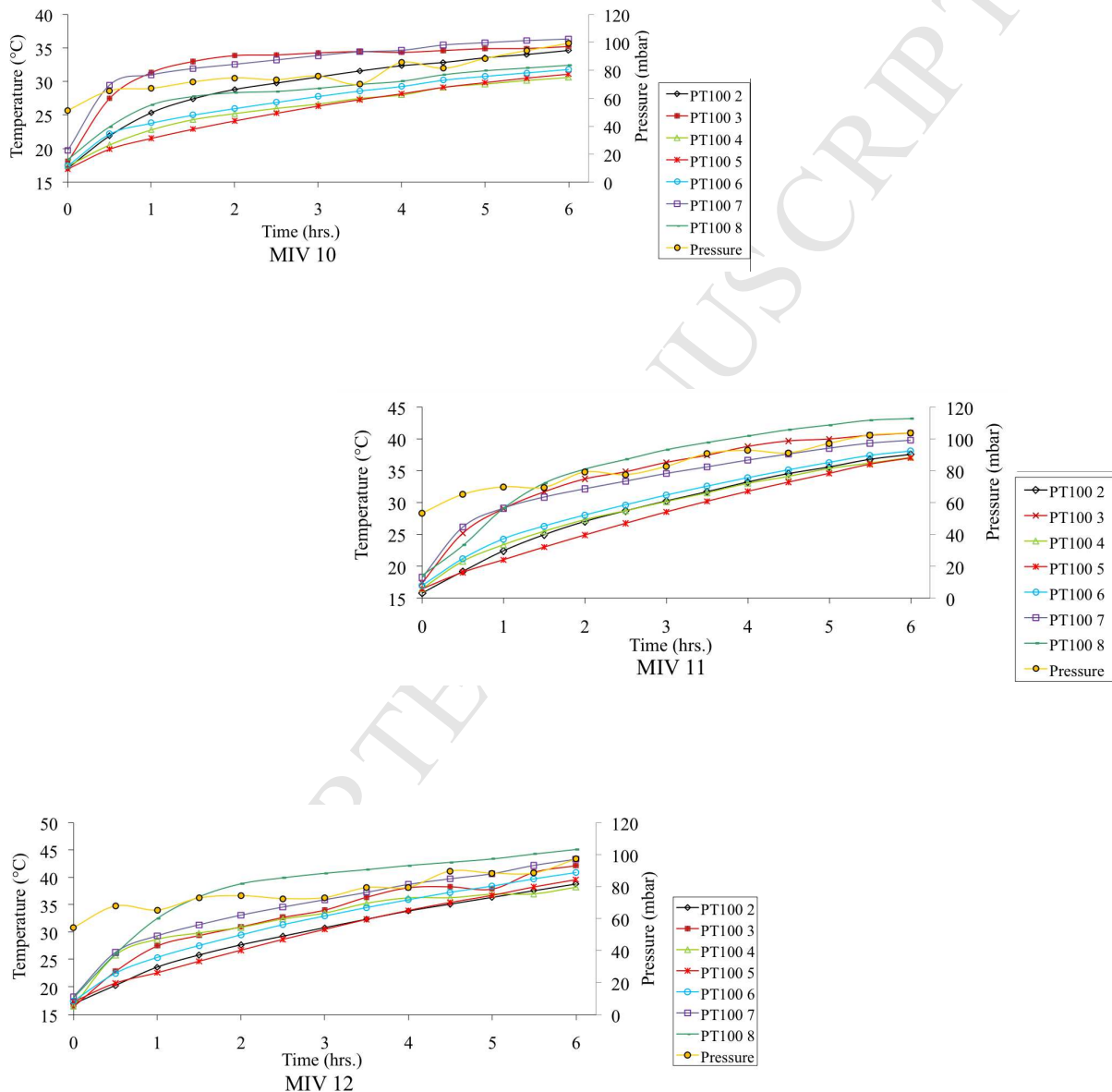
307

308

309

The inclusion of back insulation and transparent cover are crucial in achieving the desired evaporation and  
 condensation cycle. Whilst the thermal diode will operate in retaining heat during non-collection periods, unless  
 the all-important saturation temperature is achieved, the majority of heat transfer during the collection period will  
 be primarily through radiation. This is evidenced by the temperatures measured by sensor PT100 3 which is  
 located in the upper raised pocket (on the evaporator surface). In figure 7 - MIV10, the temperature at sensor  
 PT100 3 is almost constant at the latter stages of the test whilst in MIV11, the temperature at sensor PT100 3 is  
 still increasing with a slight dip at the 5 hour mark. In MIV12, the drop in temperature at sensor PT100 3 is more

310 pronounced and circled in more detail in figure 8. At the 4+ hour mark water in the pocket has completely  
 311 evaporated into the annulus but as condensate from the inner vessel starts to run back into the pocket, the  
 312 temperature starts to drop until it reaches evaporation temperature again, permitting more convective heat  
 313 transfer. A cover and some form of back insulation are therefore necessary to permit the saturation temperature in  
 314 the annulus to be attained. In the case of MIV12 this is around 38°C for the given pressure in the annulus. Further  
 315 refinements through capillary materials and coatings, covers and segmentation should enhance this process  
 316 bringing the evaporation and condensation cycle earlier resulting in better collection efficiencies.



345 Figure 7: Annulus temperatures and pressure for Mark IV selected tests over a 6 hour collection period under  
 346 solar simulation test conditions

347  
 348  
 349  
 350

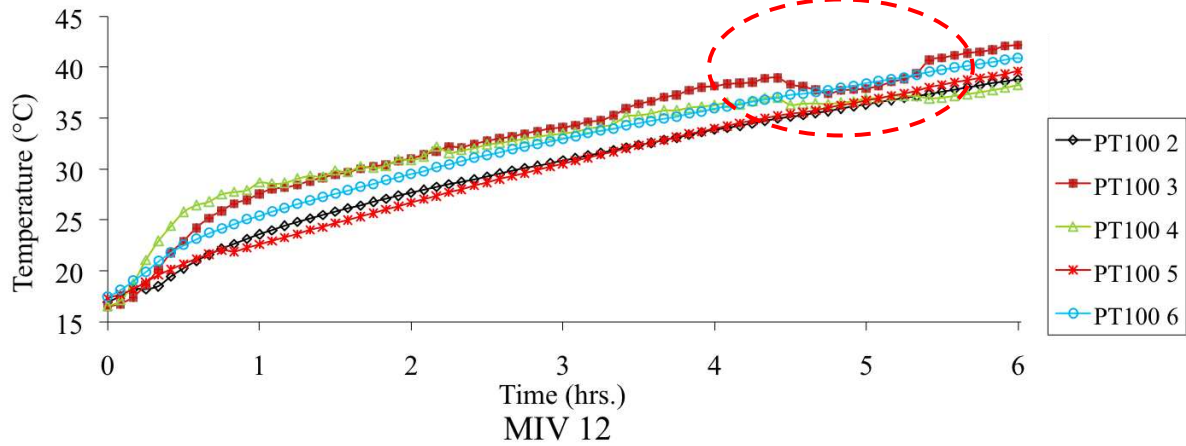


Figure 8: Annulus temperatures for MIV12 over a 6 hour collection period for selected sensors under solar simulation test conditions

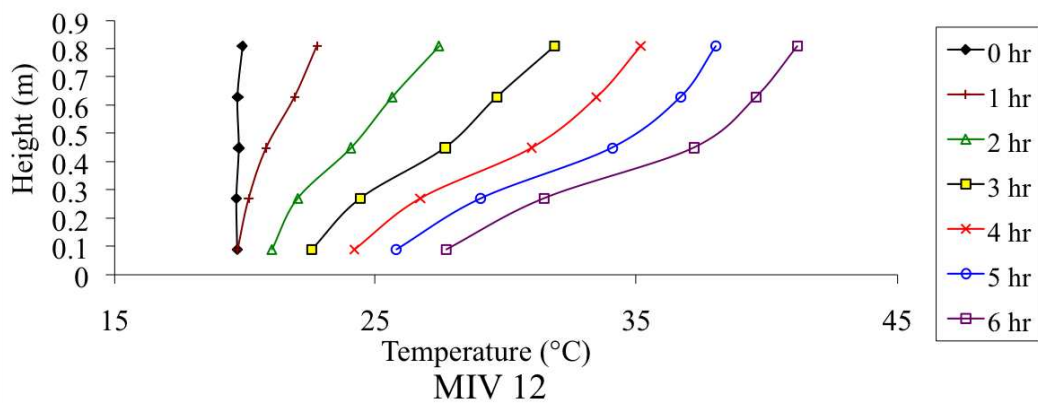
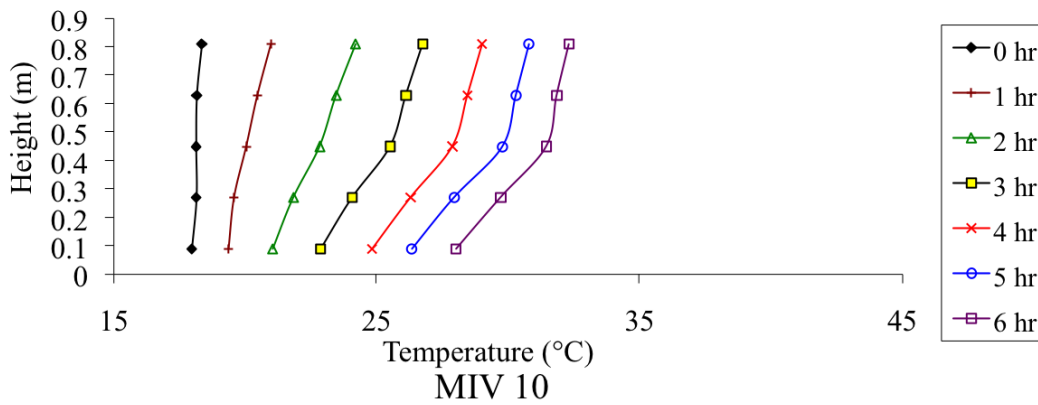


Figure 9: Hourly thermoclines during the collection period for MIV10 and MIV12 under solar simulated test conditions

Comparing the thermoclines for MIV10 and MIV12 (figure 9) and corresponding stratification index (figure 10) shows how the back insulation and transparent cover increases stratification in the thermal store. Comparing sensor PT100 8 in tests MIV10, MIV11 and MIV12 (figure 7) an 11°C increase in temperature at the top of the tank after 6 hours collection could be attributed to the inclusion of a transparent cover (MIV11) and a further 2°C due to the inclusion of the insulation in the back 1/3 of the aperture cavity (MIV12).

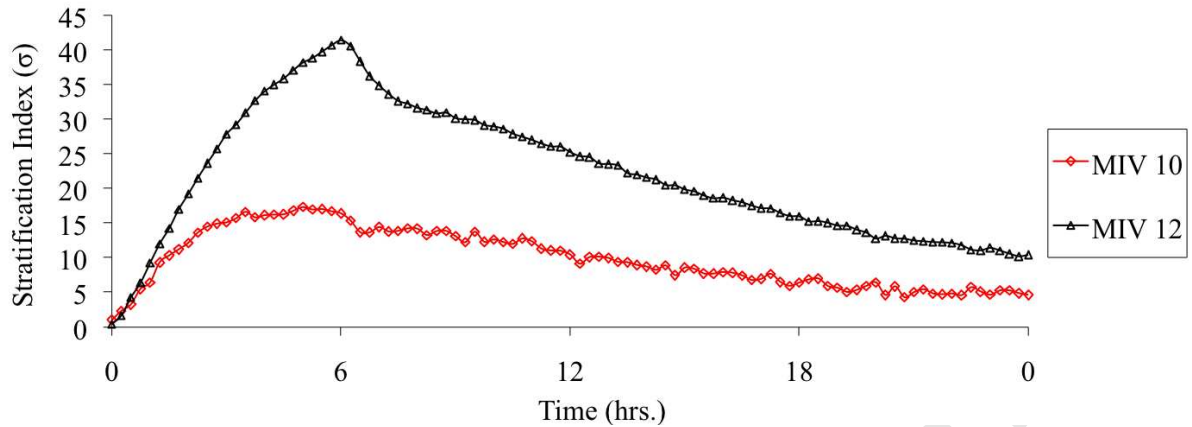


Figure 10: Stratification index for MIV10 and MIV12 over a 6 hour collection and 18 hour cool down period for solar simulated and indoor ambient test conditions

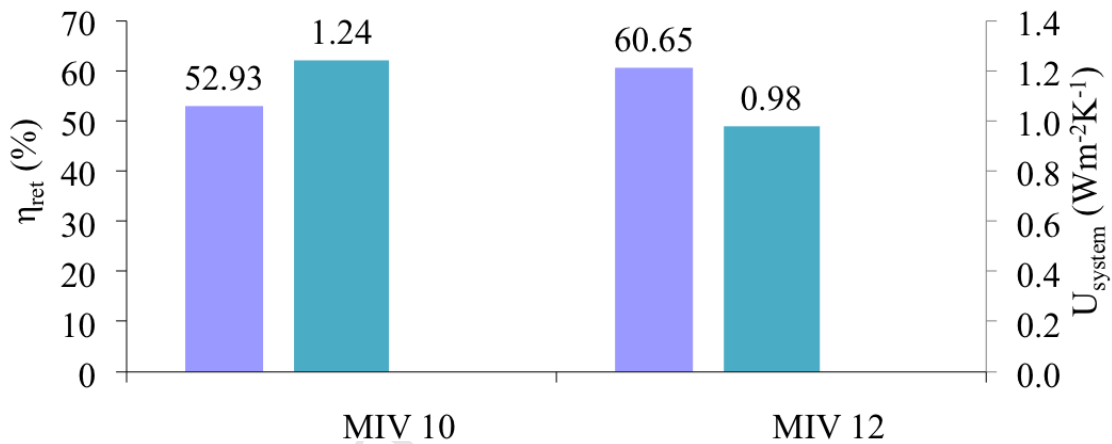


Figure 11: Heat retention efficiency and heat loss coefficient after an 18 hour cool down period for solar simulated and indoor ambient test conditions

The system 'U' value on cool down for MIV12 (figure 11) was  $0.98 Wm^{-2}K^{-1}$  an improvement of 20% ( $1.24 Wm^{-2}K^{-1}$ ) over MIV10 without the insulation and cover. The MIV12 system 'U' value was higher than that achieved in previous tests but the thermal retention for MIV12 at 60.65% was the highest retention efficiency achieved. The reduced heat losses were due to the transparent cover trapping long wave radiated heat from the ICS vessel surface and reducing convection and conduction losses from the entire ICS unit. The back insulation increases heat transfer resistance over a third of the curved surface of the ICS reducing the area over which significant heat loss from convection and conduction can take place.

## 7 Conclusions

A novel thermal diode pre-heat solar water heating system was designed and developed to be a sustainable, affordable alternative to pre-heat solar water heating systems traditionally used in DHW installations. The concept is based on the operating principles of a thermal diode using sensible/latent heat transfer, evacuation and

433 PCMs. A number of prototypes were designed, fabricated, tested and evaluated using a state-of-the-art solar  
 434 simulation test facility. Under testing, the highest 6 hour collection efficiency was 36.17% and the lowest system  
 435 'U' value was  $0.98 \text{ Wm}^{-2}\text{K}^{-1}$  (MIV12) with no draw-off. The testing highlighted the importance of cover and  
 436 insulation even in a thermal diode concept as temperatures need to be achieved and maintained to ensure the  
 437 evaporation and condensation cycle. When the current prototype ICS units are compared with other conventional  
 438 ICS systems, particularly in terms of thermal retention during non-collection periods, an improved performance is  
 439 clearly demonstrated. The measured thermal losses were approximately 40% less than other similarly measured  
 440 prototype systems,  $1.05 \text{ WK}^{-1}$  (based on  $1.08\text{m}^2$ ) to  $1.78 \text{ WK}^{-1}$  [4] and more typically greater than  $5 \text{ WK}^{-1}$  for a  
 441 commercial unit [16]. For comparison, the heat loss coefficient of a standard insulated tank is  $0.9 \text{ WK}^{-1}$ . The  
 442 study concludes that the system performance is significantly improved when the heat retaining thermal diode  
 443 feature is combined with elongated pockets and capillary matting, transparent cover, aperture cavity back  
 444 insulation and transparent aperture cover. Through experimental and parametric evaluation, a unique pre-heat  
 445 ICS solar water heating system has been designed, developed, analysed and presented. Significant steps have  
 446 been made towards a potential commercial future, but in order to fully realise this goal, much more study is  
 447 required.

448

449 Acknowledgements and Funding: This work was supported through funding from Invest Northern Ireland, Proof  
 450 of Concept scheme. Thanks to support from COST Action TU1205 Building Integrated Solar Thermal Systems.

451

## 452 NOMENCLATURE

453	$A_{\text{ap}}$	aperture area ( $\text{m}^2$ )
454	$A_{\text{unit}}$	surface area of unit ( $\text{m}^2$ )
455	$c_p$	specific heat capacity of water ( $\text{J/kgK}$ )
456	$G_{\text{ave}}$	insolation ( $\text{W/m}^2$ )
457	$m$	mass of water ( $\text{kg}$ )
458	$mc_{\text{system}}$	thermal capacity ( $\text{J/K}$ )
459	$Q_{\text{col}}$	thermal energy collected ( $\text{J}$ )
460	$Q_{\text{incident}}$	incident solar thermal energy ( $\text{J}$ )
461	$T$	temperature ( $^{\circ}\text{C/K}$ )
462	$U_{\text{system}}$	system heat loss coefficient ( $\text{W m}^{-2}\text{K}^{-1}$ )
463	$UA_{\text{system}}$	heat loss coefficient of system ( $\text{W/K}$ )
464	$\Delta t$	time (secs)
465	$\Delta T$	temperature difference ( $^{\circ}\text{C/K}$ )
466	$\eta_{\text{col}}$	collection efficiency
467	$\eta_{\text{optical}}$	optical efficiency
468	$\sigma$	stratification index
469	$\emptyset$	diameter

470

471

472 **Subscripts**

473

474 **amb** average ambient temperature475 **av** average water temperature476 **ave,heating** average water temperature averaged over the heating period (K)477 **av,b** average water temperature at bottom 1/5 of vessel478 **av,t** average water temperature at top 1/5 of vessel479 **end** average water temperature at end of heating period480 **final** average final water temperature at end of cooling period481 **initial** average initial water temperature482 **initial,c** average initial water temperature at start of cooling period483 **ret** heat loss retention484 **start** average water temperature at start of heating period

485

486

487 **REFERENCES**

488 [1] Butti K and Perlin J, 1981. A Golden Thread. Marion Boyars Publishers Ltd., London, UK

489 [2] Kemp CM, 1891. U.S. Patent No. 451384, April 28th, 1891

490 [3] Smyth M, Eames PC and Norton B, 2006. Integrated Collector Storage Solar Water Heaters. Renewable and  
491 Sustainable Energy Review, Vol. 10, Iss.6, pp 503-538492 [4] Singh R, Lazarus IJ & Souliotis M, 2016. Recent developments in integrated collector storage (ICS) solar  
493 water heaters: A review. Renewable and Sustainable Energy Reviews. Vol. 54, pp 270-298494 [5] Kalogirou S, 2014. Solar Energy Engineering - Processes and Systems. Academic Press; 2nd Edition,  
495 ISBN:978012397270496 [6] Quinlan P, 2010. The Development of a Novel Integrated Collector Storage Solar Water Heater (ICSSWH)  
497 Using Phase Change Materials and Partial Evacuation. PhD Thesis, University of Ulster, UK498 [7] Souliotis M, Quinlan P, Smyth M, Tripanagnostopoulos Y, Zacharopoulos A, Ramirez M, Yianoulis P, 2011.  
499 Heat retaining integrated collector storage solar water heater with asymmetric CPC reflector. Solar Energy, Vol.  
500 85, No. 10, pp 2474-2487501 [8] Souliotis M, Papaefthimiou S, Caouris YG, Zacharopoulos A, Quinlan, Smyth M, 2017. Integrated collector  
502 storage solar water heater under partial vacuum. Energy Vol. 139, pp 991-1002503 [9] De Beijer HA, 1998. Product Development in Solar Water Heating. Proceedings of the 5<sup>th</sup> World Renewable  
504 Energy Congress, Florence, Italy, pp 201-204, Sept. 1998505 [10] Smyth M, Quinlan P, Mondol JD, Zacharopoulos A, McLarnon D and Pugsley A, 2017. The evolutionary  
506 thermal performance and development of a novel thermal diode pre-heat solar water heater under simulated heat  
507 flux conditions. Renewable Energy Vol. 113, pp 1160-1167508 [11] Anon. Veralite 200 Technical Data Sheet , [www.iplast.be/ipb/Veralite 200 technical data sheet.pdf](http://www.iplast.be/ipb/Veralite%20technical%20data%20sheet.pdf), 9th  
509 August 2010.

510 [12] Norton B, 1992. Solar Energy Thermal Technology. Springer-Verlag, London, UK

- 511 [13] Anon., 2007a. Solar Heating – Domestic Water Heating Systems - Part 5: System Performance  
512 characterization by means of whole-system tests and computer simulation. BS ISO 9459-5:2007, British  
513 Standards Institution, London, UK
- 514 [14] Gnafakis C & Manno VP, 1989. Transient de-stratification in a rectangular enclosure. Transactions of the  
515 American Society of Mechanical Engineers, Vol. 111, pp 92 -99
- 516 [15] Visser H and Van Dijk HAL, 1991. Test procedures for short term thermal stores. Kluwer Academic  
517 Publishers, Dordrecht, Netherlands
- 518 [16] Faiman D, Hazan H, Laufer I, 2001. Reducing the heat loss at night from solar water heaters of the  
519 integrated collector–storage variety. Solar Energy Vol. 71, No. 2, pp 87–93